

A kinetic analysis of the tumor-associated galactopyranosyl-(1→3)-2-acetamido-2-deoxy- α -D-galactopyranoside antigen–lectin interaction

BANDARU NARASIMHA MURTHY and NARAYANASWAMY JAYARAMAN*

Department of Organic Chemistry, Indian Institute of Science, Bangalore 560 012

e-mail: jayaraman@orgchem.iisc.ernet.in

Abstract. A kinetic study of the tumor-associated galactopyranosyl-(1→3)-2-acetamido-2-deoxy- α -D-galactopyranoside (T-antigen) with lectin peanut agglutinin is described. The disaccharide antigen was synthesized by chemical methods and was functionalized suitably for immobilization onto a carboxymethylated sensor chip. The ligand immobilized surface was allowed interaction with the lectin peanut agglutinin, which acted as the analyte and the interaction was studied by the surface plasmon resonance method. The ligand–lectin interaction was characterized by the kinetic on-off rates and a bivalent analyte binding model was found to describe the observed kinetic constants. It was identified that the antigen–lectin interaction had a faster association rate constant (k_{a1}) and a slower dissociation rate constant (k_{d1}) in the initial binding step. The subsequent binding step showed much reduced kinetic rates. The antigen–lectin interaction was compared with the kinetic rates of the interaction of a galactopyranosyl-(1→4)- β -D-galactopyranoside derivative and a mannopyranoside derivative with the lectin.

Keywords. Antigens; carbohydrates; lectins; kinetics; surface plasmon resonance spectroscopy.

1. Introduction

Cell surface bound carbohydrates are critical in order to initiate several cellular recognition events.¹ Understanding intricate carbohydrate mediated recognition events has implications, for example, in the development of carbohydrate based diagnostics and therapeutics.² Important classes of carbohydrates are the so-called T_N , T and sT_N antigens and these are known to be tumor-associated antigens, resulting from drastic changes in the cell surface bound carbohydrates.^{3,4} The T-antigen, namely, the disaccharide galactopyranosyl-(1→3)-2-acetamido-2-deoxy- α -D-galactopyranoside, is a cancer-related marker and is a sustained target for the development of cancer vaccines.⁵ Lectins, the carbohydrate binding proteins, often serve as important tools to analyse interactions and specificities of sugar ligands at the molecular level.⁶ The lectin binding studies were conducted previously with T-antigen,^{7,8} involving the antigen specific lectin peanut agglutinin (PNA), which is a tetrameric protein, at physiological pH, having one binding site in each monomer.⁹ The

specificity and higher binding affinity of the T-antigen to the lectin originates through water-mediated hydrogen bonding between the acetamido moiety of the ligand and the amino acid residues of the lectin.⁸ In our efforts on the kinetic studies of the ligand–lectin interactions,¹⁰ a kinetic analysis of a synthetic T-antigen derivative–lectin interaction was undertaken. The analysis was performed with the aid of the surface plasmon resonance (SPR) technique, which provides information in real-time about the extent of an analyte binding to a ligand immobilized onto a surface. Interaction of glycopolypeptides carrying the T-antigen with PNA and other lectins was reported previously by Usui and co-workers, wherein, the lectins were immobilized on the surface and the polymeric ligands were used as the analyte.¹¹ The SPR studies undertaken in the present investigation on immobilized T-antigen–PNA interaction show that the association rate constant (k_{a1}) is significantly higher in the initial binding step than the subsequent binding step. The kinetic constants were compared to another lectin specific ligand, namely, galactopyranosyl-(1→4)- β -D-galactopyranoside (lactose) derivative and a non-specific mannopyranoside derivative. Details of synthesis and the binding studies are presented here.

*For correspondence

2. Experimental

2.1 General methods

Chemicals were purchased from commercial sources and were used without further purifications. Solvents were dried and distilled according to literature procedures. Analytical TLC was performed on commercial plates coated with silica gel GF254 (0.25 mm). Silica gel (100–200 mesh) was used for column chromatography. High-resolution mass spectra were obtained from a Q-TOF instrument by an electrospray ionization (ESI) technique. ^1H and ^{13}C NMR spectral analyses were performed on a spectrometer operating at 300 and 75 MHz, respectively, and the residual solvent signal was used as the internal standard. The following abbreviations were used to explain the multiplicities: *s*, singlet; *d*, doublet; *t*, triplet; *dd*, doublet of doublets; *m*, multiplet; *band*, several overlapping signals and *br*, broad. Millipore water (Milli Q-plus system, $R > 18 \text{ m}\Omega$, pH 5.5) was used to prepare the buffer solution. The buffer solution consisted of HEPES (10 mM), NaCl (150 mM) and the pH was adjusted to 7.4. Lectin PNA (salt-free lyophilized powder) was purchased from Sigma. SPR experiments were carried out on a Biacore 2000, with research grade CM5 sensor chip.

2.2 *N*-(Benzyloxycarbonyl)aminoethyl-3,4,6-tri-*O*-acetyl-2-azido-2-deoxy- α -D-galactopyranoside (**9**)

To a stirring suspension of protected amino alcohol **8** (0.170 g, 0.87 mmol), Ag_2CO_3 (0.33 g, 1.2 mmol), molecular sieves (4 Å) (0.10 g) and AgClO_4 (0.024 g, 0.12 mmol) in $\text{CH}_2\text{Cl}_2/\text{PhMe}$ (1 : 1, 15 mL), a solution of bromide 7^{13} (0.24 g, 0.6 mmol) in $\text{CH}_2\text{Cl}_2/\text{PhMe}$ (1 : 1, 10 mL) was added, under argon atmosphere and the reaction mixture was protected from light. After 12 h, the reaction mixture was diluted with CH_2Cl_2 (100 mL), filtered over celite and concentrated *in vacuo*. Purification (SiO_2 , Pet. Ether/EtOAc = 3/2) of the crude residue afforded the required α -isomer **9** (0.19 g, 61%), as a colourless viscous syrup. TLC: R_f 0.53 (Pet. Ether/EtOAc = 3 : 7). $[\alpha]_{\text{D}}^{23} + 71.0$ (*c* 2.0, CHCl_3); ^1H NMR (300 MHz, CDCl_3) δ 7.31 (app. *s*, 5H), 5.42 (*d*, 1H, $J = 2.3$ Hz), 5.35–5.33 (*m*, 2H), 5.11 (*s*, 2H), 5.00 (*d*, 1H, $J = 3.3$ Hz), 4.22 (*t*, 1H, $J = 6.6$ Hz), 4.07 (app. *d*, 2H), 3.81 (*m*, 1H), 3.66 (*dd*, 2H, $J = 3.6$ Hz, 11.1 Hz), 3.45 (*m*, 2H), 2.14 (*s*, 3H), 2.05 (*s*, 3H), 2.02 (*s*, 3H); ^{13}C NMR (100 MHz, CDCl_3) δ 170.5, 170.1,

169.9, 156.4, 136.4, 128.5, 128.1, 128.0, 127.9, 98.4, 68.2, 68.0, 67.5, 66.8, 66.7, 61.7, 57.5, 40.7, 20.6; HR-MS: calcd. for $\text{C}_{22}\text{H}_{28}\text{N}_4\text{O}_{10}$ m/z : 531.1703 $[\text{M} + \text{Na}]^+$; found: 531.1728 $[\text{M} + \text{Na}]^+$, 547.1473 $[\text{M} + \text{K}]^+$.

2.3 *N*-(Benzyloxycarbonyl)aminoethyl-3,4,6-tri-*O*-acetyl-2-acetamido-2-deoxy- α -D-galactopyranoside (**10**)

A solution of **9** (0.09 g, 0.176 mmol) in AcSH (1 mL) and pyridine (0.5 mL) was stirred at room temperature for 20 h. Removal of the solvent *in vacuo* followed by purification (PhMe/EtOAc) of the residue afforded **10** (0.083 g, 90%). TLC: R_f 0.28 (Pet. Ether/EtOAc = 3 : 7). $[\alpha]_{\text{D}}^{23} + 50.5$ (*c* 2.0, CHCl_3); ^1H NMR (400 MHz, CDCl_3) δ 7.42–7.32 (*m*, 5H), 6.08 (*d*, 1H), 5.37 (*d*, 1H, $J = 2.8$ Hz), 5.26–5.21 (*m*, 1H), 5.16 (*d*, 1H, $J = 3.2$ Hz), 5.12 (*s*, 2H), 4.90 (*d*, 1H, $J = 3.6$ Hz), 4.60 (*m*, 1H), 4.18 (*t*, 1H), 4.09 (app. *d*, 2H), 3.79–3.74 (*m*, 1H), 3.63–3.56 (*m*, 1H), 3.47–3.41 (*m*, 1H), 3.41–3.33 (*m*, 1H), 2.18 (*s*, 3H), 2.03 (*s*, 3H), 2.02 (*s*, 3H), 1.97 (*s*, 3H); ^{13}C NMR (75 MHz, CDCl_3) δ 170.9, 170.5, 170.3, 156.7, 136.2, 128.6, 128.3, 128.2, 98.3, 68.4, 68.3, 67.3, 67.0, 66.9, 62.0, 47.6, 40.9, 23.1, 20.8, 20.7, 20.6; HR-MS: calcd. for $\text{C}_{24}\text{H}_{32}\text{N}_2\text{O}_{11}$ m/z : 547.1904 $[\text{M} + \text{Na}]^+$; found: 547.1914 $[\text{M} + \text{Na}]^+$.

2.4 *N*-(Benzyloxycarbonyl)aminoethyl-4,6-benzylidene-2-acetamido-2-deoxy- α -D-galactopyranoside (**11**)

A suspension of **10** (0.25 g, 0.47 mmol) in MeOH (10 mL) was stirred in the presence of NaOMe (0.5 N) (0.5 mL). After 3 h, Amberlite IR-120 (H^+) resin was added to the reaction mixture, filtered and solvent evaporated *in vacuo* to afford the de-*O*-acetylated intermediate, as a white solid (0.18 g). The intermediate was stirred with benzaldehyde dimethyl acetal (0.2 mL) in the presence of *p*-toluene sulphonic acid (0.015 g) in DMF (3 mL) at 50°C for 2 h. The reaction mixture was added with Et_3N (0.010 mL), solvents removed *in vacuo* and the resulting crude product purified (EtOAc/MeOH = 1 : 0.05) to afford **11** (0.19 g, 83%), as a white solid. TLC: R_f 0.10 (EtOAc). $[\alpha]_{\text{D}}^{23} + 65.0$ (*c* 1.0, CHCl_3); ^1H NMR (300 MHz, CDCl_3) δ 7.53–7.49 (*m*, 5H), 7.37–7.30 (app. *s*, 5H), 6.56 (*d*, 1H, $J = 7.5$ Hz), 5.52 (*s*, 1H), 5.29 (*m*, 1H), 5.11 (*q*, 2H), 4.94 (*d*, 1H, $J = 3.3$ Hz), 4.40 (*ddd*, 1H, $J = 3.6$ Hz, 8.7 Hz,

11.1 Hz), 4.21 (*d*, 1H, $J = 12.6$ Hz), 4.09 (*d*, 1H, $J = 2.7$ Hz), 3.98 (*d*, 1H, $J = 11.8$ Hz), 3.81 (*m*, 1H), 3.71 (*m*, 1H), 3.59 (*s*, 1H), 3.42 (*m*, 2H), 3.30 (*m*, 2H), 2.00 (*s*, 3H); ^{13}C NMR (75 MHz, CDCl_3) δ 172.1, 156.9, 137.5, 136.3, 129.2, 128.6, 128.3, 128.2, 128.1, 126.3, 101.2, 98.6, 75.5, 69.0, 67.9, 66.9, 63.1, 50.2, 40.8, 23.1; HR-MS: calcd. for $\text{C}_{25}\text{H}_{30}\text{N}_2\text{O}_8$ m/z : 509.1900 $[\text{M} + \text{Na}]^+$; found: 509.1889 $[\text{M} + \text{Na}]^+$.

2.5 Aminoethyl- β -D-galactopyranosyl-(1 \rightarrow 3)-2-acetamido-2-deoxy- α -D-galactopyranoside (T-antigen derivative) (1)

A solution of **11** (0.103 g, 0.212 mmol) in PhMe/MeNO₂ (1 : 1, 8 mL) was stirred for 1 h at room temperature and in the absence of light. After removal of approximately half of the solvent *in vacuo*, 2,3,4,6-tetra-*O*-benzoyl- α -D-galactopyranosyl bromide¹⁵ (0.31 g, 0.47 mmol) and Hg(CN)₂ (0.12 g, 0.47 mmol) were added under argon atmosphere and stirred for 20 h. The reaction mixture was diluted with EtOAc (20 mL), washed with aq. KI (1 N), followed by brine. The organic layer was dried (Na₂SO₄), concentrated *in vacuo* and purified (EtOAc/PhMe = 7 : 3) to afford protected derivative of the disaccharide **1** (0.20 g, 87%). TLC: R_f 0.23 (Pet. Ether/EtOAc = 2/3). $[\alpha]_{\text{D}}^{23} + 96.5$ (*c* 2.0, CHCl_3); ^1H NMR (300 MHz, CDCl_3) δ 8.04 (*d*, 2H, $J = 8.4$ Hz), 7.92 (*d*, 2H, $J = 7.3$ Hz), 7.87 (*d*, 2H, $J = 7.2$ Hz), 7.70 (*d*, 2H, $J = 7.2$ Hz), 7.56–7.13 (band, 22H), 5.91 (*d*, 1H, $J = 3.1$ Hz), 5.73 (*dd*, 1H, $J = 7.6$ Hz, 10.2 Hz), 5.66 (*d*, 1H, $J = 9.5$ Hz), 5.52 (*dd*, 1H, $J = 3.2$ Hz, 10.2 Hz), 5.32 (*s*, 1H), 5.08–4.96 (band, 5H), 4.66 (*m*, 1H), 4.46 (*ddd*, 1H, $J = 3.4$, 7.2, 10.9 Hz), 4.33 (*m*, 3H), 4.04 (*m*, 2H), 3.65 (*m*, 2H), 3.44–3.22 (band, 4H), 1.63 (*s*, 3H); ^{13}C NMR (75 MHz, CDCl_3) δ 170.3, 166.1, 165.6, 165.5, 165.1, 156.5, 137.5, 136.4, 135.8, 130.0–126.0, 101.8, 100.8, 98.5, 75.5, 75.3, 71.8, 71.7, 70.2, 69.2, 68.1, 67.9, 66.8, 63.1, 48.5, 40.8, 23.2; HR-MS: calcd. for $\text{C}_{59}\text{H}_{56}\text{N}_2\text{O}_{17}$ m/z : 1087.3477 $[\text{M} + \text{Na}]^+$; found: 1087.3622 $[\text{M} + \text{Na}]^+$, 1103.3363 $[\text{M} + \text{K}]^+$.

A solution of the above protected disaccharide (0.24 g, 0.23 mmol) and CSA (0.05 g) in MeOH (10 mL) were stirred for 2 h and Et₃N (100 μl) was added to neutralize CSA and solvents removed. Purification of the crude product (EtOAc/Pet. Ether = 7 : 3) afforded 4,6-de-*O*-benzylidenated product (0.21 g, 96%), as a gummy solid. A suspension of the pro-

ected disaccharide obtained above (0.20 g, 0.2 mmol) in MeOH (15 mL) and Pd/C (10%) (0.025 g) was subjected to hydrogenolysis for 24 h. After filtration over celite, the solvents were removed *in vacuo* to afford the benzyloxycarbonyl group deprotected product, as a white foamy solid. The product was dissolved in MeOH and admixed with NaOMe/MeOH (0.5 M, 0.1 mL) and left stirring for 12 h, neutralized with Amberlite IR-120 resin (H^+ form), filtered and the filtrate concentrated *in vacuo*. The resulting solid was triturated with EtOAc and dried to afford **1** (0.09 g, 95%). $[\alpha]_{\text{D}}^{23} + 52.3$ (*c* 0.6, H₂O); ^1H NMR (400 MHz, D₂O) δ 4.74 (*d*, 1H, $J = 3.6$ Hz), 4.23 (*d*, 1H, $J = 7.2$ Hz), 4.05 (*d*, 1H, $J = 2.8$ Hz), 3.95 (*d*, 1H, $J = 2.8$ Hz), 3.86–3.30 (band, 10H), 3.23–3.02 (band, 4H), 1.67 (*s*, 3H); ^{13}C NMR (75 MHz, D₂O) δ 174.6, 101.2, 97.7, 75.6, 74.8, 73.3, 71.3, 69.2, 66.9, 65.1, 63.4, 61.8, 49.3, 40.1, 22.3; HR-MS: calcd. for $\text{C}_{16}\text{H}_{30}\text{N}_2\text{O}_{11}$ m/z : 449.1747 $[\text{M} + \text{Na}]^+$, found: 449.1747 $[\text{M} + \text{Na}]^+$.

2.6 Aminoethyl- β -D-galactopyranosyl-(1 \rightarrow 4)- β -D-glucopyranoside (lactose derivative) (2)

To a stirring suspension of protected amino alcohol **8** (0.49 g, 2.5 mmol), Hg(CN)₂ (0.63 g, 2.5 mmol), HgBr₂ (0.46 g, 1.2 mmol) and molecular sieves (4 Å) in CH₂Cl₂ (30 mL), a solution of benzobromolactose¹⁵ (2.9 g, 2.5 mmol) in CH₂Cl₂ (5 mL) was added drop-wise, over a period of 10 min. The mixture was stirred until TLC analysis (Pet. ether/EtOAc = 3 : 2) showed disappearance of the bromide. Work-up and purification (SiO₂, Pet. ether/EtOAc = 3 : 2) of the crude residue afforded the *O*-benzoyl-protected **2** (2.30 g, 74%), as a colourless viscous syrup. TLC: R_f 0.48 (Pet. ether/EtOAc = 3 : 2). $[\alpha]_{\text{D}}^{23} + 51.0$ (*c* 1.0, CHCl_3); ^1H NMR (300 MHz, CDCl_3) δ 8.17–7.99 (*m*, 12H), 7.83 (*d*, 2H, $J = 8.1$ Hz), 7.65–7.19 (*m*, 26H), 5.95–5.86 (*m*, 2H), 5.57 (app *t*, 2H), 5.30 (*br s*, 1H), 5.18–4.95 (*m*, 3H), 4.73–4.71 (app *d*, 2H), 4.62 (*dd*, 1H, $J = 3.9$ Hz, 12.0 Hz), 4.36 (*t*, 1H, $J = 9.3$ Hz), 4.05 (*t*, 1H, $J = 6.5$ Hz), 3.92–3.70 (*m*, 5H), 3.38 (*m*, 2H); ^{13}C NMR (75 MHz, CDCl_3) δ 169.8, 166.0, 165.5, 165.0, 156.4, 137.9, 136.8, 133.5, 130.5–128.1, 125.5, 101.5, 101.1, 76.1, 73.4, 73.0, 72.1, 71.6, 70.3, 69.5, 67.9, 66.6, 62.6, 61.4, 41.0. MALDI-TOF MS: calcd. for $\text{C}_{71}\text{H}_{61}\text{NO}_{20}\text{Na}$ m/z : 1271.23 $[\text{M} + \text{Na}]^+$, found: 1271.4 $[\text{M} + \text{Na}]^+$.

A suspension of *O*-benzoyl-protected **2** (0.72 g, 0.54 mmol) in EtOAc/MeOH (1 : 1, 50 mL) and

Pd/C (10%) (0.3 g) was subjected to hydrogenolysis for 16 h. After filtration over celite, the solvents were removed *in vacuo*. The resulting white foamy solid was dissolved in MeOH/THF (1 : 1, 10 mL) and admixed with NaOMe/MeOH (0.5 M, 1 mL), left stirring for 12 h, neutralized with Amberlite IR-120 resin (H⁺ form), filtered and the filtrate concentrated *in vacuo*. The resulting solid was triturated with EtOAc, Me₂CO and dried to afford **2** (0.19 g, 90%), as a gummy solid. [α]_D²³ + 39.2 (*c* 1.0, H₂O); ¹H NMR (300 MHz, D₂O) δ 4.38 (*d*, 1H, *J* = 7.5 Hz), 4.29 (*d*, 1H, *J* = 7.5 Hz), 3.98–3.1 (band, 16H); ¹³C NMR (75 MHz, D₂O) δ 103.7, 102.7, 78.9, 76.1, 75.0, 73.4, 73.2, 71.7, 69.3, 66.6, 61.8, 60.7, 49.7, 40.2; HR-MS: calcd. for C₁₄H₂₇NO₁₁ *m/z*: 386.1662 [M + Na]⁺, found: 386.1666 [M + Na]⁺.

2.7 Aminoethyl- α -D-mannopyranoside (**3**)

To a stirring suspension of protected amino alcohol **8** (0.86 g, 4.4 mmol), Hg(CN)₂ (1.11 g, 4.4 mmol), HgBr₂ (0.79 g, 2.2 mmol) and molecular sieves (4 Å) in CH₂Cl₂ (25 mL), a solution of benzobromomannose¹⁵ (3.0 g, 4.5 mmol) in CH₂Cl₂ (5 mL) was added drop-wise over a period of 10 min. The reaction mixture was stirred until TLC analysis (Pet. ether/EtOAc = 3 : 2) showed a complete disappearance of the bromide. Work-up and purification (SiO₂, Pet. ether/EtOAc = 3 : 2) of the crude residue afforded *O*-benzoyl-protected **3** (3.08 g, 91%), as a colourless viscous syrup. TLC: *R_f* 0.62 (Pet. ether/EtOAc = 3/2). [α]_D²³ + 72.0 (*c* 2.0, CHCl₃); ¹H NMR (300 MHz, CDCl₃) δ 8.05 (*d*, 2H, *J* = 7.5 Hz), 8.01 (*d*, 2H, *J* = 7.8 Hz), 7.93 (*d*, 2H, *J* = 7.8 Hz), 7.77 (*d*, 2H, *J* = 7.8 Hz), 7.64–7.21 (*m*, 17H), 5.98 (*app. d*, 1H, *J* = 3.3 Hz), 5.75 (*dd*, 1H, *J* = 7.8 Hz, 10.3 Hz), 5.60 (*dd*, 1H, *J* = 10.3 Hz, 3.6 Hz), 5.16 (*br s*, 1H), 5.03 (*q*, 1H, *J* = 12.3 Hz), 4.92 (1/2 AB *q*, 1H, *J* = 12.3 Hz), 4.80 (*d*, 1H, *J* = 7.8 Hz), 4.64 (*dd*, 1H, *J* = 6.6 Hz, 11.4 Hz), 4.43 (*dd*, 1H, *J* = 6.0 Hz, 11.4 Hz), 4.31 (*t*, 1H, *J* = 6.6 Hz), 3.99 (*m*, 1H), 3.75 (*m*, 1H), 3.41 (*m*, 2H); ¹³C NMR (75 MHz, CDCl₃) δ 165.9, 165.5, 165.4, 136.5, 133.6, 133.3, 133.2, 129.9–128.0, 101.8, 71.5, 69.8, 69.8, 68.0, 65.2, 62.0, 40.8; HR-MS: calcd. for C₄₄H₃₉NO₁₂ *m/z*: 796.2370 [M + Na]⁺; found: 796.2341 [M + Na]⁺.

A suspension of *O*-benzoyl-protected **3** (1.0 g, 1.3 mmol) in EtOAc/MeOH (1 : 1, 20 mL) and Pd/C (10%) (0.2 g) was hydrogenolysed for 12 h. After

filtration over celite, the solvents were removed *in vacuo* to afford a white foamy solid. The foamy solid was dissolved in MeOH (20 mL) and admixed with NaOMe/MeOH (0.5 M) (1 mL), left stirring for 12 h, neutralized with Amberlite IR-120 resin (H⁺ form), filtered and the filtrate concentrated *in vacuo*. The resulting solid was triturated with EtOAc, Me₂CO and dried to afford **3** (0.26 g, 92%), as a gummy solid. [α]_D²³ + 33.0 (*c* 1.0, MeOH); ¹H NMR (300 MHz, D₂O) δ 4.75 (*br s*, 1H), 3.85–3.5 (band, 6H), 3.23–3.02 (band, 4H); ¹³C NMR (75 MHz, D₂O) δ 100.7, 73.7, 72.4, 71.1, 67.4, 64.1, 61.4, 39.8; HR-MS: calcd. for C₈H₁₇NO₆ *m/z*: 246.0954 [M + Na]⁺, found: 246.0938 [M + Na]⁺.

2.8 SPR experiments

2.8a Immobilization of sugar ligands onto CM5 sensor chip: After equilibration of the CM5 sensor surface with HEPES buffer (pH 7.4), the surface was activated with NHS in H₂O (0.1 M) and EDC in H₂O (0.1 M).¹⁶ The ligand **1** was injected, at a concentration of 2 mg/mL in NaOAc buffer (pH 4.3) (10 mM), with a flow rate of 5 μ L/min. To obtain a sufficient amount on the surface, the ligand was injected 4 times and after each injection, a gradual increase in response was observed. After coupling, remaining NHS esters were blocked by the addition of ethanolamine hydrochloride (1.0 M) (pH 8.5) for 3 min. The stability of immobilized ligand surface was checked by injection of 10 mM NaOH, buffer solution and 10 mM glycine-HCl. In this manner, approximately 220 RU of **1** on Fc2, 210 RU of **2** on Fc3 and 195 RU of **3** on Fc4 were immobilized covalently on the CM5 surface. The surface with mannose derivative **3** was used as a reference to the T-antigen **1** and lactose **2** immobilized surfaces.

2.8b Kinetic experiments for ligand-PNA interactions: All binding experiments with lectin PNA was performed at a flow rate of 20 μ L/min using HEPES buffer as the eluant. The studies were performed in HEPES buffer (10 mM) (pH 7.4) containing NaCl (150 mM) and at 298 K. Injection times of PNA were 300 s, followed by 300 s dissociation phase. Regeneration was performed with 30 s pulse of HCl (100 mM). For the calculations of the kinetic constants, PNA was diluted in HEPES buffer ranging from the concentrations of 1, 2, 4, 8 and 16 μ M. The PNA was diluted in the running buffer (HEPES, pH 7.4) to minimize the bulk effects attributable to changes in the refractive index of the solution. Each

PNA solution was injected into channel 2 (T-antigen derivative **1**), channel 3 (lactose derivative **2**) and channel 4 (mannopyranoside derivative **4**). The specific response of the PNA towards **1** or **2** was obtained by subtracting the channel 4 response from either channel 2 or channel 3 response, respectively. The mass transfer limitations were checked after each kinetic experiment and mass transfer effects were found to be negligible. Sensorgram analysis of each ligand-lectin interactions was performed with the BIAevaluation software.¹⁸ The sensorgrams were fitted to the kinetic models and the kinetic constants were derived from the global fit of the data to these models. The association rate constant for the second step of the interaction (k_{a2}) in the bivalent model analysis was obtained in the unconventional unit of $\text{RU}^{-1}\text{s}^{-1}$. The unit of k_{a2} , $1/\text{RUs}$ is modified to $1/\text{Ms}$ by the following expression: $k_{a2} (1/\text{Ms}) = k_{a2} (1/\text{RUs}) \times 100 \times \text{molecular weight of PNA}$.¹⁹

3. Results and discussion

Immobilization of the sugar ligands onto the sensor chip was desired, which required accordingly the functionalization of the ligands. For immobilization onto the carboxymethylated dextran coated sensor surface, the sugar ligands were functionalized with an amine functionality. Apart from the T-antigen derivative (**1**), a lactose derivative (**2**) and a mannopyranoside derivative (**3**) were utilized in the study.

Figure 1 presents the structures of the sugar ligands, tethered with the amine functionality.

3.1 Synthesis of the ligands 1–3

Synthesis of derivative **1** was initiated from galactopyranose (**4**), which was transformed to 3,4,6-tri-*O*-acetyl galactal (**5**)¹² and subsequently to 3,4,6-tri-*O*-acetyl-2-azido-2-deoxy-D-galactopyranosyl nitrate **6** and the bromide **7**¹³ (scheme 1).

Glycosylation of the aglycosyl acceptor **8** with the bromide **7**, in the presence of $\text{Ag}_2\text{CO}_3/\text{AgClO}_4$ promoters, led to the formation of the glycosylated product **9** (scheme 2), with the α -anomer in 61% yield and the β -anomer in about 35% yield.

The α -anomer **9** was treated with AcSH in pyridine¹⁴ to afford the acetamido product **10**, which was de-*O*-acetylated and converted to 4, 6-*O*-benzylidene-ated product **11**, having a free hydroxyl group at C-3. Glycosylation of **11** with benzobromogalactose,¹⁵ in the presence of Hg(II), followed by deprotections in sequence of the (i) benzylidene group; (ii) benzyloxycarbonyl group and (iii) acetyl groups led to the isolation of the T-antigen derivative **1** (scheme 2).

The preparation of the lactose derivative **2** and the mannopyranosyl derivative **3** were accomplished through glycosylation using either benzobromolactose or benzobromomannose¹⁵ and protected ethanolamine **8**, in the presence of Hg(II) promoters. Deprotections of the protecting groups led to the

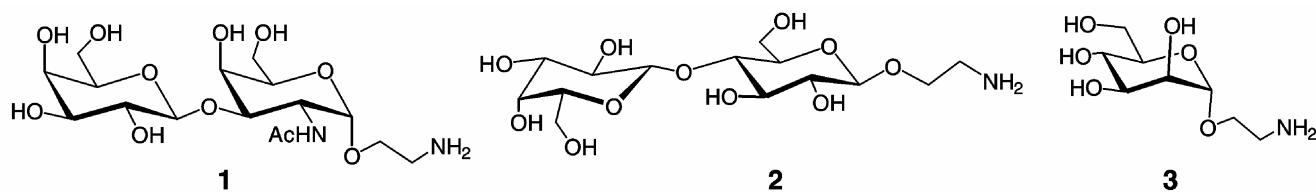
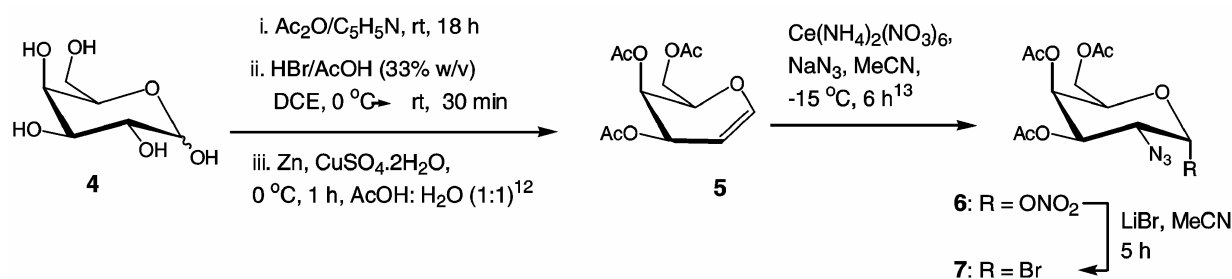
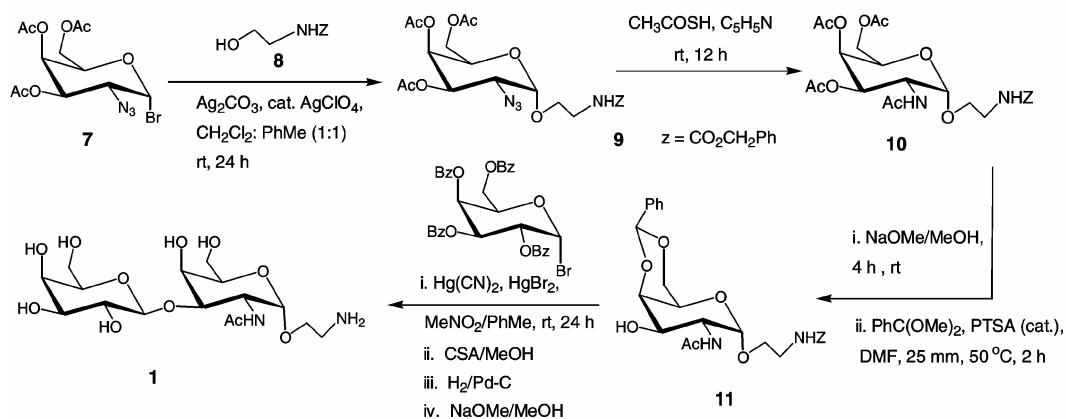


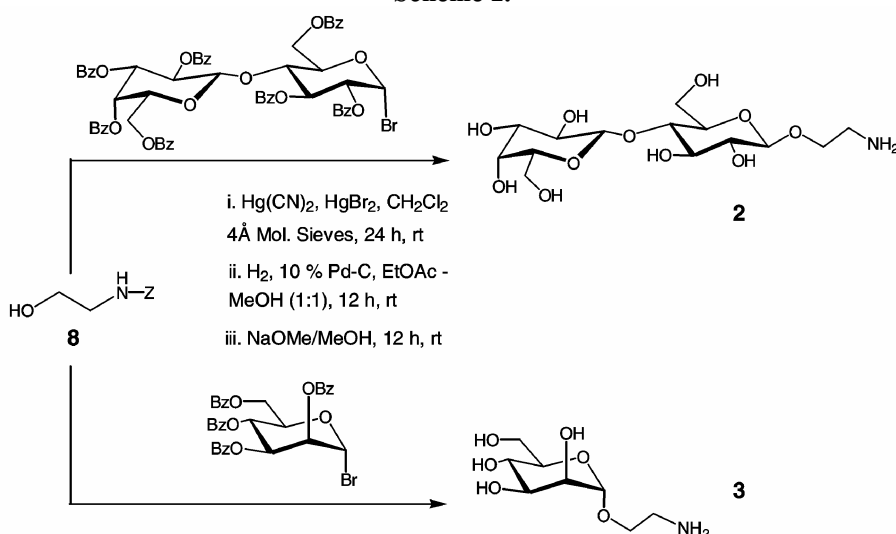
Figure 1. Structures of sugar ligands 1–3.



Scheme 1.



Scheme 2.



Scheme 3.

formation of the free hydroxyl group containing **2** and **3** (scheme 3). The newly formed glycosyl derivatives **1–3** were characterized by spectroscopic and spectrometric methods.

3.2 Kinetic studies of the interactions of the glycosyl derivatives **1–3** with lectin PNA by the SPR method

The ligand–lectin interaction profiles were monitored with the aid of the SPR technique. The SPR method provides real-time monitoring of the complexation process and conducting the kinetic assays of the complexation. The responses to adsorption and desorption processes that occur are recorded in a sensorgram, as a function of time. The subsequent use of a simulation software allows fitting the ob-

served data with a kinetic model, thereby allowing calculation of the kinetic association (k_a) and dissociation (k_d) rate constants or the equilibrium constant (K). The method warrants that the limitations arising due to mass transport phenomena and non-specific interactions are diminished, in order to eliminate the artifacts during the analysis. The kinetic studies were performed on a BIAcore 2000 system (Biacore AB, Uppsala, Sweden), using a carboxymethylated dextran coated (CM5) sensor chip. The ligands **1–3** were immobilized onto the CM5 chip, using *N*-hydroxysuccinimide (NHS)–*N*-ethyl-*N'*-(3-dimethyl aminopropyl)carbodiimide hydrochloride (EDC) mediated coupling of the amino group of the ligand with the carboxylic acid functionalities on the sensor surface.¹⁶ A low surface density of the ligand immobilization was maintained (~200 RU).

The lectin PNA was brought in solution as analyte into the flow system and was allowed interaction with the immobilized ligands. The flow cell containing immobilized mannopyranoside ligand served as the reference to determine the non-specific binding. Figure 2 presents the sensorgrams of the interactions of PNA with the immobilized ligands 1–3. A considerably higher response was observed for the T-antigen 1-PNA interaction, when compared to 2-PNA interaction. The mannopyranoside ligand 3 did not show the response for the lectin, reflecting the known non-interacting nature of the ligand to the lectin.¹⁷ The significantly higher response unit for the T-antigen 1-lectin interaction is also in agreement with the solution phase studies.⁸

The kinetic study of the immobilized ligand–lectin interactions was performed at five concentrations, ranging from 1 μM to 16 μM . The complexation was followed for 300 s and subsequently, the buffer solution, without the analyte, was passed over the surface for 300 s to dissociate the complex. Upon dissociation of the complex, the ligand immobilized surface was regenerated by using a 60 s pulse of HCl (100 mM, pH 2.4). Figure 3 presents the sensorgrams obtained at five different concentrations for the T-antigen 1-lectin and 2-lectin interactions. A visual inspection of the sensorgrams shows that the 1-lectin interaction exhibits a faster association and a slower dissociation than that of the 2-lectin interaction. In order to assess the mass transfer limitations, a fixed concentration of the lectin (8 μM) was passed over the T-antigen derivative (1)

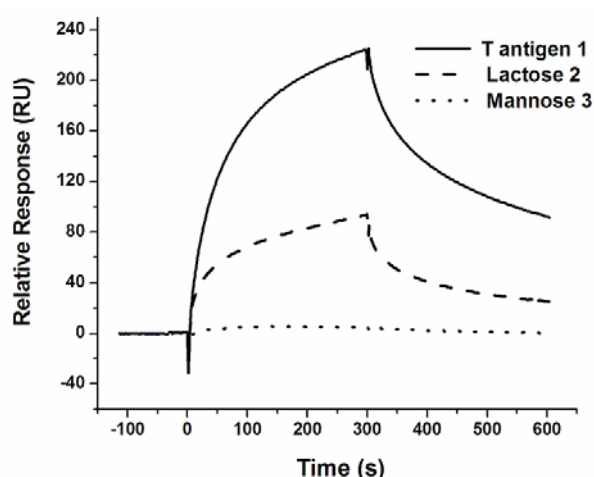


Figure 2. The relative responses obtained for the binding of PNA to T-antigen derivative 1, lactose derivative 2 and mannose derivative 3 at a particular PNA concentration (16 μM).

immobilized surface, at flow rates of 5, 25 and 75 mL min^{-1} and the observed binding profiles were found to be independent of the flow rates, thereby eliminating the mass transfer effects during the ligand–lectin interactions. The binding curves, namely, the sensorgrams, obtained for the ligand–lectin interactions were fitted to kinetic models, using the BIAevaluation programme¹⁸ and the fitting was judged from the χ^2 values, that denote how closely the model fits with the observed data. A kinetic model with a low χ^2 value ($\chi^2 < 10$) is considered to provide a good fitting with the observed data. With the kinetic models analysed, it was found that the bivalent analyte binding model provided the best fit with the observed data than other models. With the bivalent analyte binding model describing the ligand–lectin interaction better, two association and dissociation rate constants were obtained for the first and second steps of the binding processes, according to the equation $A + B \leftrightarrow AB$; $AB + B \leftrightarrow AB_2$, where A and B denote the lectin and ligand, respectively. The results of the kinetic analysis resulting from the bivalent analyte binding model are given in table 1. The bivalent analyte binding model for the T-antigen 1-lectin interaction showed that the first association rate constant (k_{a1}) was much higher (i.e. rapid first association) than the second association rate constant (k_{a2}). This indicates faster saturation of the lectin binding by the ligand in the initial binding step, leading to reduced ligand–lectin complexation in the subsequent step. In contrast, the lactose 2-lectin interaction exhibited an equivalent magnitude of the association rate constants for both the steps (k_{a1} and k_{a2}), indicating the importance of a two-step process in the binding of the lectin to the immobilized lactose derivative 2. The dissociation rate constants for the first (k_{d1}) and second (k_{d2}) steps showed a similar magnitude for both the ligands 1 and 2.

However, considering the association rate constants, it is seen that 1-lectin complex exhibits a slower dissociation rate constant for the first step than that for the 2-lectin complexation. This trend indicates that (i) the T-antigen 1-lectin complexation has a rapid association rate constant and a slower dissociation rate constant and (ii) the lactose derivative 2 binds to the lectin slowly and subsequently, the ligand–lectin complex dissociated relatively faster.

The main driving force for the complexation resides in the initial binding event, characterized by k_{a1} and k_{d1} , as the initial binding event is far more

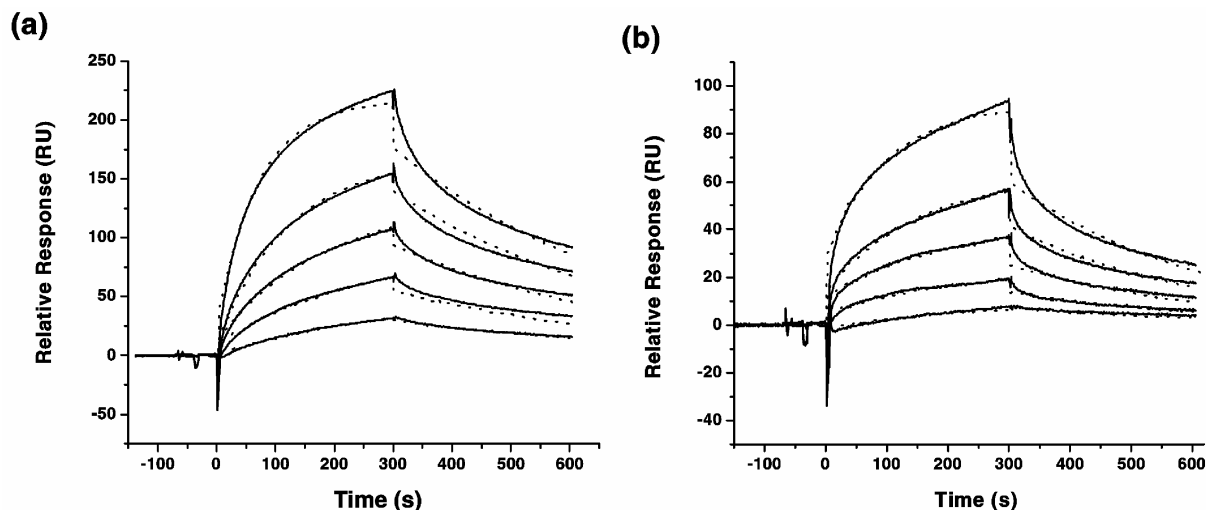


Figure 3. The sensorgrams of the interaction of PNA with (a) T-antigen derivative **1** and (b) lactose derivative **2**, at PNA concentrations of 1, 2, 4, 8 and 16 μM (bottom to top). The solid lines represent the experimental data and dotted lines represent the global fits of the data to a bivalent analyte binding model.

Table 1. Kinetic data for the binding of PNA to T-antigen **1** and lactose **2** derivatives at 25°C.

Sugar ligand	Bivalent analyte binding analysis				
	k_{a1} ($\text{M}^{-1} \text{s}^{-1}$)	k_{d1} (s^{-1})	k_{a2} ($\text{M}^{-1} \text{s}^{-1}$)	k_{d2} (s^{-1})	χ^2
T-antigen (1)	9.77×10^2	2.32×10^{-2}	9.74×10^1	1.65×10^{-3}	2.4
Lactose (2)	1.69×10^2	2.47×10^{-2}	1.21×10^2	1.86×10^{-3}	0.8

important than the subsequent binding events. The association constants (K_{a1}), calculated as k_{a1}/k_{d1} , were found to be $4.2 \times 10^4 \text{ M}^{-1}$ and $6.8 \times 10^3 \text{ M}^{-1}$ for the T-antigen **1**-lectin and lactose derivative **2**-lectin complexations, respectively. These K_{a1} values for the immobilized ligand-lectin complexes are slightly higher when compared to those known previously from the solution phase studies on un-derivatized T-antigen-PNA and lactose-PNA interactions,⁸ having K_a values of $2.4 \times 10^4 \text{ M}^{-1}$ and $2.0 \times 10^3 \text{ M}^{-1}$, respectively.

The important outcome of the kinetic studies presented here is the identification of the faster association rate constant in the initial binding event of the T-antigen **1**-lectin interaction and the considerably reduced association rate constant in the subsequent step of the complexation. The faster association rate constant (k_{a1}) is also coupled with slower dissociation rate constant (k_{d1}). In contrast, the lactose derivative **2**, which is also specific to the lectin PNA, has a weaker association rate constant (k_{a1}) in the initial binding process and a relatively faster dissociation

rate constant (k_{d1}). The subsequent binding process also has an association rate constant (k_{a2}) of similar magnitude as the first binding step, thereby indicating the contributions of both the steps in the ligand-lectin interaction.

4. Conclusion

In conclusion, synthesis of amine-tethered T-antigen disaccharide derivative (**1**), a lactose derivative (**2**) and a mannopyranoside derivative (**3**) were accomplished and these derivatives were immobilized onto a CM5 sensor surface suitable for the kinetic analysis of the ligand-lectin binding behaviour. Lectin PNA was used to determine the kinetics of the ligand-lectin complexations. A bivalent analyte binding model was found to be suitable to fit the kinetic analysis. From the studies, it is identified that the T-antigen **1**-lectin interaction is nearly saturated in the initial step of binding (k_{a1}), whereas the lactose derivative **2** binds to the lectin with comparable association rate constants for both the initial and sub-

sequent binding steps (k_{a1} and k_{a2}). The results of the present study may bear importance for a better understanding of the ligand–lectin interactions relevant to ligand types that result from acute biological aberrations.

Acknowledgement

The authors thank the Department of Science and Technology (DST), New Delhi, for financial support. NMB thanks Council of Scientific and Industrial Research (CSIR), New Delhi, for a research fellowship.

References

1. (a) Varki A 1993 *Glycobiology* **3** 97; (b) Karlsson K A 1995 *Curr. Opin. Struct. Biol.* **5** 622
2. (a) Toyokuni T and Singhal A K 1995 *Chem. Soc. Rev.* **24** 231; (b) Wong C-H 2003 *Carbohydrate-based drug discovery* (Wiley-VCH Weinheim)
3. Hakomori S 1991 *Curr. Opin. Immunol.* **43** 646
4. (a) Springer G F 1984 *Science* **224** 1198; (b) Itzkowitz S H, Yuan M, Montgomery C K, Kjeldsen T, Takahashi H K, Bigbee W L and Kim Y S 1989 *Cancer Res.* **49** 197
5. (a) Livingston P O, Koganty R, Longenecker B M, Lloyd K O and Calves M 1992 *Vaccine Res.* **1** 99; (b) Chen Y, Jain R K, Chandrasekaran E V and Matta K L 1995 *Glycoconj. J.* **12** 55; (c) Hung Y S, Madej M, Koganty R R and Longenecker B M 1990 *Cancer Res.* **50** 4308
6. Lis H and Sharon N 1998 *Chem. Rev.* **98** 637
7. (a) Baek M-G and Roy R 2002 *Bioorg. Med. Chem.* **10** 11; (b) Gabius H-J, Schoster C, Gabius S, Brinck U and Tietze L-E 1990 *J. Histochem. Cytochem.* **38** 1625; (c) Weimar T, Bukowski R and Young N M 2000 *J. Biol. Chem.* **275** 37006
8. (a) Pratap J V, Bradbrook G M, Reddy G B, Surolia A, Raftery J, Helliwell J R and Vijayan M 2001 *Acta Crystallogr.* **D57** 1584; (b) Reddy G B, Srinivas V R, Ahmad N and Surolia A 1999 *J. Biol. Chem.* **274** 4500; (c) Swamy M J, Gupta D, Mahanta S K and Surolia A 1991 *Carbohydr. Res.* **213** 59
9. Pereira M E A, Kabat E A, Lotan R and Sharon N 1976 *Carbohydr. Res.* **51** 107
10. (a) Murthy B N, Sampath S, Jayaraman N 2005 *Langmuir* **21** 9591; (b) Murthy B N, Voelcker N H, Jayaraman N 2006 *Glycobiology* **16** 822; (c) Murthy B N, Jayaraman N, Sinha S, Surolia A and Indi S S 2007 *Glycoconjugate J.* (in press).
11. Zeng X, Nakaaki Y, Murata T and Usui T 2000 *Arch. Biochem. Biophys.* **383** 28
12. Tomonaga F, Yago K, Zen S, Sato T, Nonaka N, Yoshida T, Tajima H, Sato M, Okamoto N, Yamamoto S, Takizawa M, Nagura K, Hirooka M, Asami K and Koto S 1999 *Bull. Chem. Soc. Jpn.* **72** 765
13. Lemieux R U and Ratcliffe R M 1979 *Can. J. Chem.* **57** 1244
14. Shanguan N, Katukojvala S, Greenberg R and Williams L J 2003 *J. Am. Chem. Soc.* **125** 7754
15. (a) Fletcher Jr H G 1963 *Methods Carbohydr. Chem.* **2** 226; (b) Ness R K, Fletcher Jr H G and Hudson C S 1950 *J. Am. Chem. Soc.* **72** 2200
16. *BIAapplication hand book* Pharmacia Biosensor AB Uppsala, Sweden 1994
17. Pereira M E A, Kabat E A, Lotan R and Sharon N 1976 *Carbohydr. Res.* **51** 107
18. *BIAevaluation software and BIAevaluation Handbook* BIAcore Uppsala Sweden 1998
19. (a) Kristian M M, Katja M A and Andreas P 1998 *Anal. Biochem.* **19** 397; (b) Bernet J, Mullick J, Panse Y, Parab P B and Sahu A 2004 *J. Virology* **78** 9446